Influenza A virus reassortment in mammals gives rise to genetically distinct within-host sub-populations

Ketaki Ganti[1], Anish Bagga[2], Lucas M. Ferreri[1,3], Ginger Geiger[3], Silvia Carnaccini[3], C. Joaquin Caceres[3], Brittany Seibert[3], Yonghai Li[4], Liping Wang[5], Taeyong Kwon[4], Yuhao Li[4], Igor Morozov[4], Wenjun Ma[5,6], Juergen A. Richt[4,6], Daniel R. Perez[3,7], Katia Koelle[8,9] and Anice C. Lowen[1,9*]

[1]Department of Microbiology and Immunology, Emory University School of Medicine, Atlanta, GA, USA

[2]Emory College of Arts and Sciences, Atlanta, GA, USA

[3]Department of Population Health, Poultry Diagnostic and Research Center, College of Veterinary Medicine, University of Georgia, Athens, GA, USA

[4]Department of Diagnostic Medicine and Pathobiology, College of Veterinary Medicine, Kansas State University, Manhattan, KS, USA

[5]Department of Veterinary Pathobiology, and Department of Molecular Microbiology and Immunology, University of Missouri, Columbia, MO, USA

[6]St. Jude Center of Excellence for Influenza Research and Response (SJ-CEIRR)

[7] The Center for Research on Influenza Pathogenesis and Transmission (CRIPT-CEIRR)

[8]Department of Biology, Emory University, Atlanta, GA

[9]Emory Center of Excellence for Influenza Research and Response (Emory-CEIRR)

*anice.lowen@emory.edu

Summary

Influenza A virus (IAV) genetic exchange through reassortment has the potential to accelerate viral evolution and has played a critical role in the generation of multiple pandemic strains. For reassortment to occur, distinct viruses must co-infect the same cell. The spatio-temporal dynamics of viral dissemination within an infected host therefore define opportunity for reassortment. Here, we used wild type and synonymously barcoded variant viruses of a pandemic

H1N1 strain to examine the within-host viral dynamics that govern reassortment in guinea pigs, ferrets and swine. The first two species are well-established models of human influenza, while swine are a natural host and a frequent conduit for cross-species transmission and reassortment. Our results show reassortment to be pervasive in all three hosts but less frequent in swine than in ferrets and guinea pigs. In ferrets, tissue-specific differences in the opportunity for reassortment are also evident, with more reassortants detected in the nasal tract than the lower respiratory tract. While temporal trends in viral diversity are limited, spatial patterns are clear, with heterogeneity in the viral genotypes detected at distinct anatomical sites revealing extensive compartmentalization of reassortment and replication. Our data indicate that the dynamics of viral replication in mammals allow diversification through reassortment but that the spatial compartmentalization of variants likely shapes their evolution and onward transmission.

Introduction

Influenza A viruses (IAVs) have a broad host range, with the greatest diversity in wild bird species and established lineages circulating in poultry, swine, humans and other mammalian hosts[1,2]. Host range for a given lineage is restricted by species barriers to infection, but occasional spillover events can result in sustained transmission, seeding new lineages[3,4]. Establishment of novel IAVs in humans is the source of influenza pandemics and has major ramifications for public health and the economy[5,6]. Reassortment of gene segments between IAVs adapted to distinct host species can give rise to chimeric viruses with enhanced potential for cross-species transfer[7]. Prominent examples include the reassortant strains that gave rise to the 1957, 1968 and 2009 influenza pandemics[8,9].

Among non-human mammalian species, swine are of particular interest. Transmission of IAV between swine and humans is relatively common, due not only to an extensive interface in agricultural settings, but also to similarities between pigs and humans in the host factors that support viral replication[10,11]. Swine hosts are also somewhat susceptible to infection with avian IAV, creating the opportunity for co-infection and reassortment of viruses that are typically separated by host species barriers[12]. For this reason, swine are often referred to as mixing vessels for IAV reassortment[13,14]. The role of swine in the 2009 influenza pandemic[9], and the abundant

59 reassortment that characterizes IAV in swine[15-19], offer ample support for this designation.
60 Although the central position of swine in IAV ecology and evolution is well understood[10,13,16] , the
61 within-host viral dynamics that govern reassortment in this host are less well characterized.
62 We have previously reported that IAV reassortment occurs frequently *in vivo,* although frequency
63 varies with virus strain and host species[20-24]. Here, we used three mammalian systems to evaluate
64 how viral population structure within the host shapes genotypic diversity generated through
65 reassortment. The hosts examined comprise guinea pigs, ferrets and pigs. While pigs are an
66 important natural host, guinea pigs and ferrets are well-characterized models for human IAV[25-
67 27]. To monitor reassortment in the absence of selection pressures, we coinfected each animal
68 with wild type and synonymously barcoded variant viruses of a pandemic H1N1 (pH1N1) strain
69 background[28]. We find that co-infection at the cellular level is extensive and reassortant viruses
70 are consistently observed in both upper and lower respiratory tracts throughout the course of
71 infection. In ferrets, markedly greater viral genotypic diversity is generated in the upper
72 respiratory tract compared to the lower tract. Viral populations at these two sites are
73 furthermore highly dissimilar genetically, revealing strong spatial compartmentalization.
74 Diversity generated through reassortment in swine is generally lower than in guinea pigs and
75 ferrets and, as in ferrets, viral diversity in swine is characterized by extensive spatial
76 compartmentalization. Taken together, our data reveal spatial structure within the mammalian
77 respiratory tract to be a major factor defining the extent of IAV diversity engendered through
78 reassortment.
79
80 **Results**
81 **Viral genotypic diversity generated through reassortment in the mammalian nasal tract**
82 To evaluate the viral genotypic diversity generated via reassortment, guinea pigs, ferrets and pigs
83 were coinfected with well-matched parental viruses of the influenza A/Netherlands/602/2009
84 (NL09; pH1N1) background. Termed wild type (WT) and variant (VAR), these coinfecting viruses
85 differ by a single synonymous mutation introduced into each gene segment of the VAR virus and
86 distinct epitope tags encoded in the hemagglutinin open reading frame of each virus. Following
87 determination of the 50% infectious dose (ID_{50}) of the virus mixture in ferrets and utilizing prior

88 ID_{50} results in guinea pigs[29], reassortment in these species was analyzed at two doses (1×10^2 and
89 1×10^5 ID_{50}). In pigs, a single dose of 2×10^6 PFU was used.
90 To monitor reassortment in the upper respiratory tract, nasal samples were collected
91 longitudinally, and the genotypes of clonal isolates derived from each sample were determined.
92 The parental origin of each of the eight segments was defined, allowing identification of all 254
93 possible reassortant genotypes and both parental genotypes. Here, a genotype is defined as a
94 constellation of eight gene segments and any nucleotide diversity present is not considered.
95 Reassortment was detected in all samples from all species tested (Supp Fig 1). To characterize
96 the viral diversity generated through reassortment, we calculated the frequency of unique
97 genotypes, frequency of parental genotypes, richness and Shannon-Weiner diversity for each
98 sample (Fig 1).
99 In all three host species, the same reassortant virus is rarely detected across multiple time points
100 (Supp Fig 1), suggesting genotypic loss due to stochastic processes. Parental genotypes (WT or
101 VAR), however, are consistently detected in the nasal samples of each animal in at least two time
102 points, (Fig 1B, F, J, M). Since 21 viral isolates were genotyped from each sample, richness has a
103 maximum value of 21 in our dataset. Richness is often high in guinea pigs and ferrets, with values
104 ranging from 4 to 18, while the range in pigs falls between 3 and 10 (Fig 1C, G, K, N). Trends in
105 diversity correspond to those of richness (Fig 1D, H, L, O). Comparison across all time points
106 shows significantly higher richness and diversity in guinea pigs and ferrets than in pigs (Fig 1N, O;
107 $p<0.01$, ANOVA). Taken together, these results reveal that the mammalian respiratory tract
108 presents an environment with high potential for the generation of viral diversity via
109 reassortment.

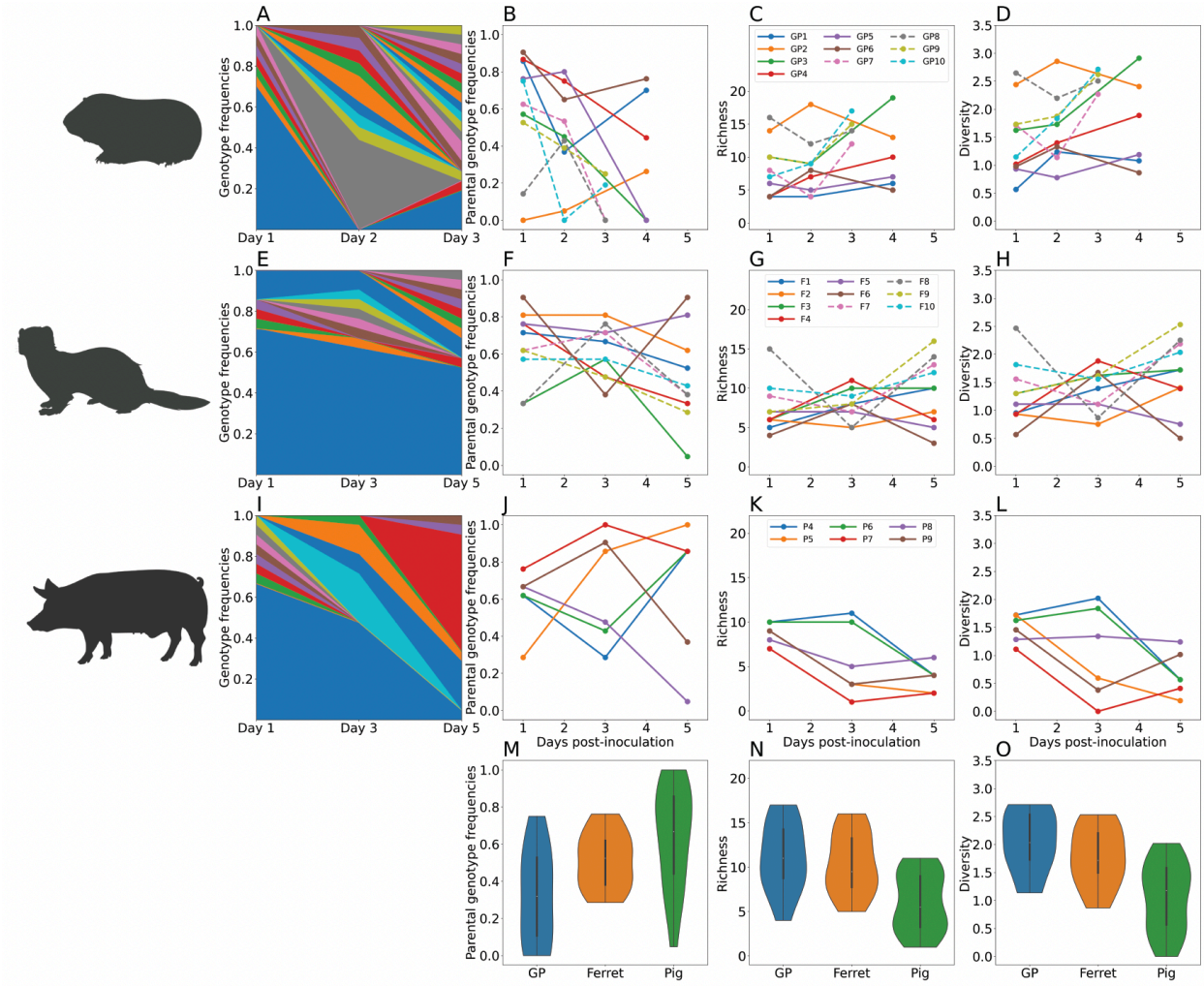

Figure 1: Viral genotypic diversity generated through reassortment in the mammalian nasal tract. *Results from guinea pigs are shown in panels A–D, ferrets in panels E–H and swine in panels I-L. Stacked plots (A, E, I) show frequencies of unique genotypes detected in one representative animal over time. Blue and orange represent the WT and VAR parental genotypes, respectively. Frequency of both parental genotypes combined (B, F, J), richness (C, G, K) and Shannon-Weiner diversity (D, H, L) are each plotted as a function of time. Guinea pigs and ferrets inoculated at high dose ($1x10^5$ ID_{50}) and low dose ($1x10^2$ ID_{50}) are indicated with dashed and solid lines, respectively. The distribution of parental genotype frequencies (M), richness (N) and diversity (O) across all time points in each species is shown with violin plots. Differences in richness and diversity between swine and guinea pigs and between swine and ferrets were significant (p<0.01,*

121 *ANOVA). Parental genotype frequencies differed significantly between swine and guinea pigs*
122 *(p=0.003, ANOVA), and were not significant between swine and ferrets (ANOVA).*
123
124 **Viral diversity generated through reassortment is greater in the ferret nasal tract than in the**
125 **lungs.** In mammalian hosts, IAV replication can be distributed throughout the respiratory tract.
126 Using the ferret model, we compared the extent of viral diversity arising through reassortment
127 in upper and lower respiratory tracts. Nasal turbinates and lung tissues were collected on days 1,
128 2, 3 or 4 from ferrets inoculated with $1x10^2$ or $1x10^5$ ferret ID_{50}. Genotyping of viral isolates
129 revealed that the number of unique genotypes detected is routinely higher in nasal turbinates
130 compared to lung at both doses (Fig 2A–C). Similarly, Shannon-Weiner diversity in nasal
131 turbinates is typically higher than in the lung (Fig 2D). These differences in both richness and
132 diversity are significant (Fig 2E, F) ($p=8.6x10^{-5}$ and p=0.0014, respectively; paired t-test).
133 We hypothesized that the distinct outcomes of co-infection in the upper and lower respiratory
134 tracts were indicative of little viral dispersal between the two sites. To test this hypothesis, we
135 modeled free mixing between the lung and nose by computationally shuffling intact genotypes
136 between the two tissues. We then compared our observed data to the resultant simulated
137 dataset (Fig 2C, D). This approach revealed that richness and diversity seen in the lungs is low
138 relative to that expected for free mixing, with observed values typically falling below the 5th
139 percentile of simulated results. In contrast, richness and diversity observed in nasal turbinates is
140 typically above the mean. This analysis suggests that spread of virus between upper and lower
141 respiratory locations occurs relatively rarely, such that abundant diversity generated through
142 reassortment in the nasal tract does not seed a similarly diverse population in the lungs.

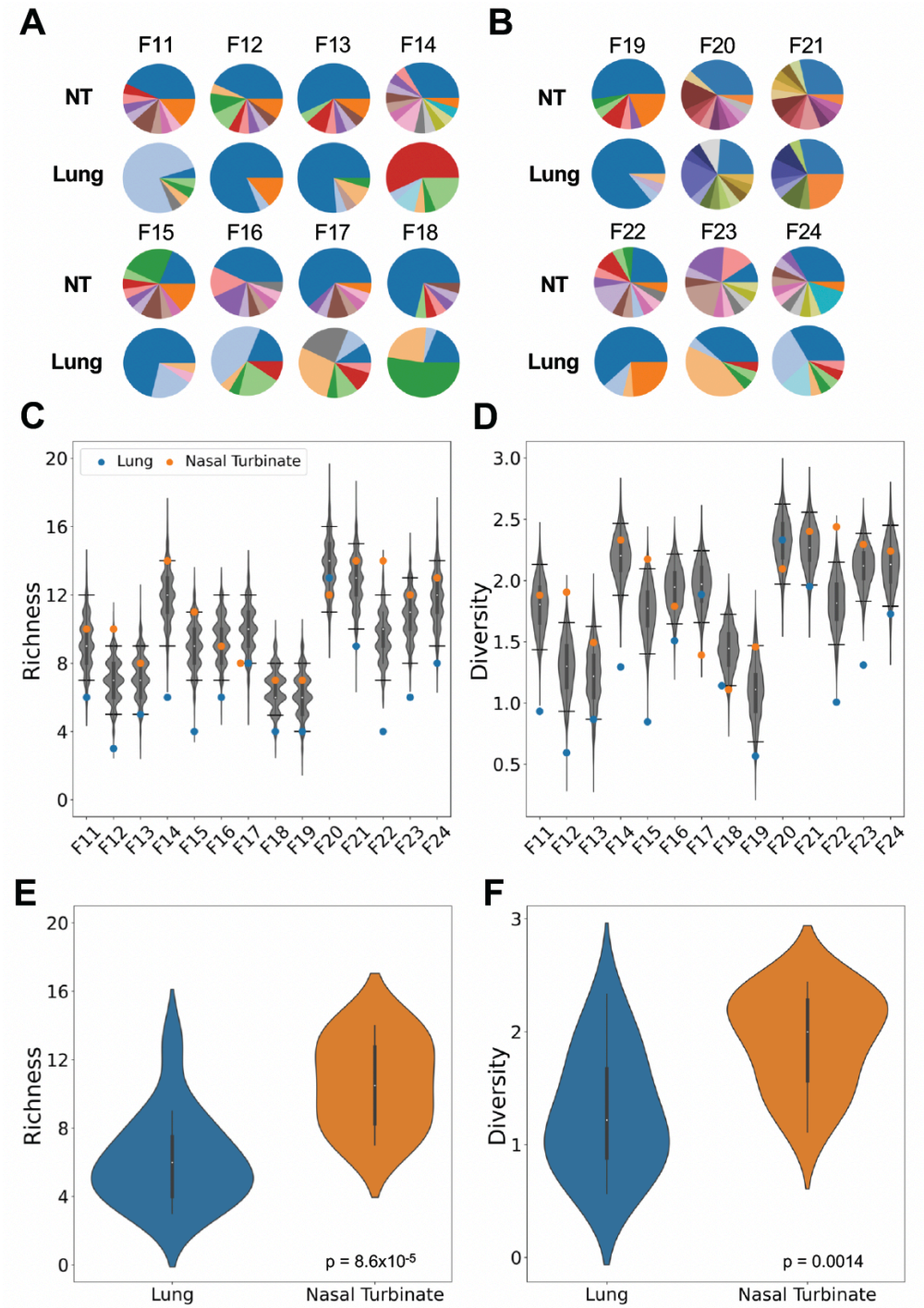

Figure 2: Viral diversity generated through reassortment is greater in the ferret nasal turbinates than in the lungs. *Pie charts show frequencies of unique genotypes detected in the nasal turbinates (NT) and lung of ferrets inoculated with $1x10^2$ FID_{50} (A) or $1x10^5$ FID_{50} (B), with the blue and orange sections representing WT and VAR parental genotypes, respectively. Richness (C) and*

148 *diversity (D) are plotted, with observed results (colored points) overlaid on the distribution of*
149 *simulated data (grey violins). Dashed lines denote the 95th and 5th percentiles. The distribution of*
150 *richness (E) and diversity (F) in NT and lungs of all individuals is shown with violin plots. Differences*
151 *between NT and lungs were significant by both measures (p<0.01, paired t-test).*
152
153 **Reassortant viral populations in the ferret upper and lower respiratory tracts are distinct**.
154 Examination of the specific genotypes identified in the nasal turbinates and lung within a given
155 ferret revealed almost no overlap (Fig 2A, B). To more rigorously assess this apparent dissimilarity
156 of viral populations, we calculated normalized beta diversity (β_n) between pairs of samples[30]. This
157 dissimilarity metric has a range between 0 and 1, with a beta value of 0 indicating that two
158 samples are identical in their genotype composition and frequencies, and a beta value of 1
159 indicating no genotypic overlap. In all ferrets, high beta diversities of >0.5 are seen between nasal
160 turbinate and lung samples of the same animal (Fig 3A). Indeed, beta diversity values calculated
161 between pairs of samples within and between ferrets indicate that the nasal and lung viral
162 populations within an individual are typically as distinct as populations replicating in different
163 animals (Fig 3A). To test whether a lack of viral dispersal between anatomical sites could account
164 for this observation, we compared the observed beta diversity to the distribution of beta diversity
165 values obtained from the computational simulation of free mixing outlined above. For most
166 ferrets, observed beta diversity falls above the 95th percentile of the distribution (Fig 3B). Thus,
167 the highly distinct viral populations seen in nasal and lung tissues are inconsistent with free
168 mixing between these sites. These data further support the notion that virus replicating within
169 the ferret upper and lower respiratory tracts form distinct compartments, with reassortment
170 occurring independently at the two sites.
171 To visualize the spatial distribution of coinfecting viruses within ferret tissues, the tagged HA
172 proteins of WT and VAR origin were stained within lung and nasal tissue sections (Fig 3C). This
173 analysis revealed that microscopic fields that are positive for viral antigen tend to show a high
174 density of infected cells at both tissue sites. Strikingly, most infected cells are positive for both
175 WT and VAR antigens, indicating high levels of viral co-infection within the host, consistent with
176 the robust reassortment observed.

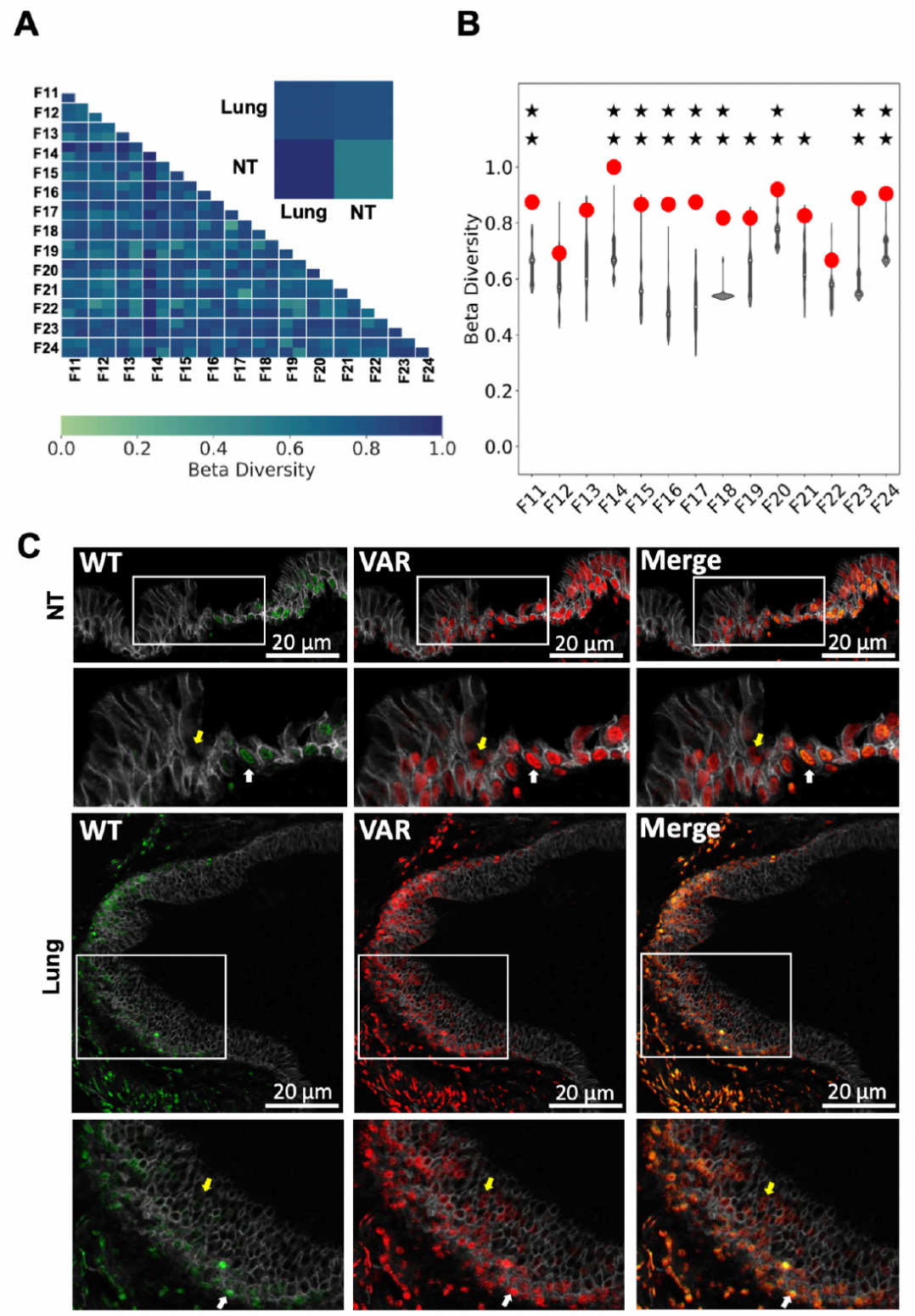

Figure 3: Reassortant viral populations in the ferret upper and lower respiratory tracts are distinct. *Heat map showing normalized beta diversity of viral populations in ferret lung and nasal*

180 *turbinates (NT) (A). The inset shows a representative comparison between the tissues of ferrets*
181 *F23 and F21, to indicate the position of NT and lung within the matrix. Normalized beta diversity*
182 *is plotted in (B) with observed results (colored points) overlaid on the distribution of simulated*
183 *data (gray violins). One star indicates that observed data is above the 95th percentile of the*
184 *distribution; two stars indicates that observed data is above the 99th percentile. (C)*
185 *Immunohistochemistry images of ferret NT and lung sections stained for WT (green) and VAR*
186 *(red) viruses at day 3 post-inoculation. Gray staining marks epithelial cell borders. Yellow coloring*
187 *in merged images indicates the presence of both WT and VAR HA antigens in the same cell.*
188 *Zoomed insets of both NT and lung sections are shown with white arrows indicating co-infected*
189 *cells and yellow arrows indicating singly infected cells.*
190
191 **Local diversity arising through reassortment is modest within the swine respiratory tract.**
192 Analysis of nasal swabs showed limited genotypic diversity in the swine nasal tract. We expanded
193 this investigation of reassortment in pigs by sampling the nasal tract and each of the seven lung
194 lobes of groups of three pigs on day 3 or 5 post-inoculation. Viral titers in the nasal tract of these
195 animals on day 3 were insufficient to support analysis of reassortment. Genotype frequencies
196 observed from the remaining sites were plotted and overlaid on a schematic of a pig lung (Fig 4A-
197 F). Although one or more reassortants are detected in all but three of the 45 samples, the viral
198 populations tend to carry high proportions of parental virus. At a minority of sites, a specific
199 reassortant is predominant. Richness is less than 10 for most samples (Fig 4G) and Shannon-
200 Weiner diversities less than 1.0 are common (Fig 4H). Thus, overall, the diversity generated
201 through reassortment throughout the swine respiratory tract is moderate. To evaluate the extent
202 to which a lack of viral mixing across the sampled locations limits richness and diversity, we
203 compared the observed results to those expected if viruses mix freely throughout the respiratory
204 tract (Fig 4G, H). To simulate free mixing, we randomly sampled intact viral genotypes from all
205 those detected within a given pig. The resultant richness and Shannon-Weiner diversity values
206 show wide distributions. However, much of the observed data lies below the 5th percentile of
207 these distributions, suggesting that pockets of low richness and diversity persist locally due to an

absence of mixing across anatomical sites. In sum, local genotypic diversity generated via reassortment is modest throughout the swine respiratory tract.

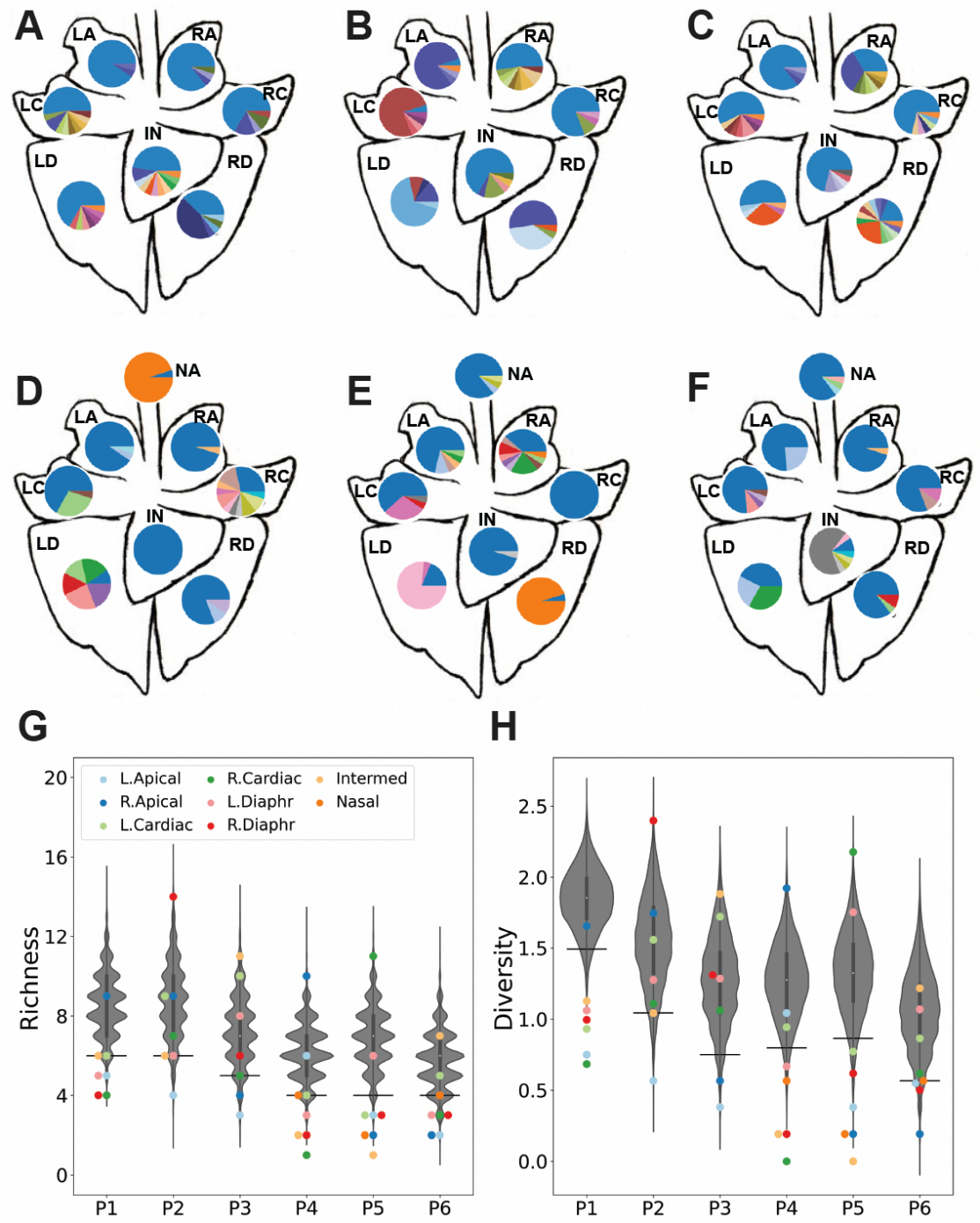

Figure 4: Local diversity arising through reassortment is modest within the swine respiratory tract. *Pie charts showing frequencies of unique genotypes present within each lung lobe of a given*

214 *pig on day 3 (A-C) and the nasal tract and each lung lobe of a given pig on day 5 (D-F) with blue*
215 *and orange sections representing WT and VAR parental genotypes, respectively. The tissue sites*
216 *are abbreviated as NA-Nasal; LA-Left Apical; RA-Right Apical; LC-Left Cardiac; RC-Right Cardiac;*
217 *LD-Left Diaphragmatic; RD-Right Diaphragmatic; IN-Intermediate. Simulated richness (G) and*
218 *diversity (H) are plotted, with observed results (colored points) overlaid on the distribution of*
219 *simulated data (grey violins). Dashed lines denote the 95th and 5th percentiles.*
220
221 **Reassortant viral populations show extensive compartmentalization within the swine**
222 **respiratory tract.** Examination of the reassortant viral genotypes identified in swine tissues
223 reveals little to no overlap across locations within an individual animal (Fig 4A-F). We again used
224 beta diversity to assess the similarity of viral populations in a pairwise and quantitative manner.
225 As seen in ferrets, beta values in pigs were typically high (Fig 5A and Supp Fig 2). Indeed, viral
226 populations sampled from within a pig were as distinct from one another as those sampled from
227 different pigs (Fig 5A). To test whether a lack of viral dispersal between anatomical sites could
228 account for this observation, we compared the beta diversity observed for a pair of locations
229 within a pig to the distribution of beta diversity values obtained from a simulation of free mixing
230 between those locations (Fig 5B and Supp Fig 3). For most pairs of tissues, the observed data are
231 at the high extreme of this distribution, falling within the 95th percentile of the simulated results.
232 Thus, spatial compartmentalization within the swine respiratory tract is extensive.
233 To visualize the spatial distribution of co-infecting viruses within swine tissues, the tagged HA
234 proteins of WT and VAR origin were stained (Fig 5C and Supp Fig 4). As in ferrets, a high density
235 of infected cells is visible in regions positive for viral antigen and most infected cells are positive
236 for both WT and VAR viruses. Thus, the high levels of viral co-infection observed in ferrets extends
237 to swine.

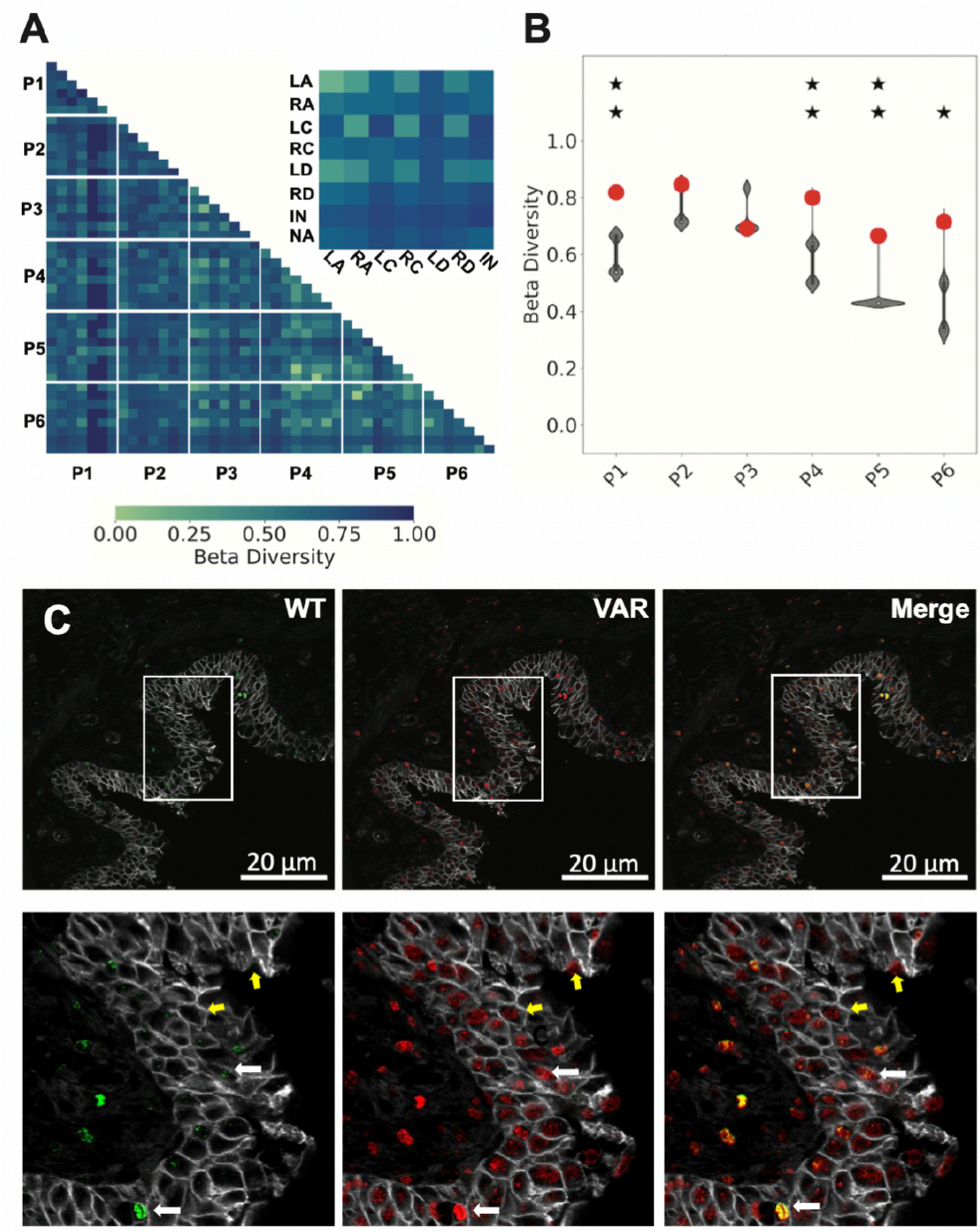

Figure 5: Reassortant viral populations show extensive compartmentalization within the swine respiratory tract. *Heat map showing normalized beta diversity of viral populations in swine lung and nasal tract (A). The inset shows a representative comparison between the tissues of pigs P3 and P6, to indicate the position of each tissue within the matrix. The tissue sites are abbreviated*

243 *as NA-Nasal; LA- Left Apical; RA- Right Apical; LC-Left Cardiac; RC-Right Cardiac; LD-Left*
244 *Diaphragmatic; RD-Right Diaphragmatic; IN-Intermediate. Normalized beta diversity between*
245 *the left apical and left cardiac lobes is plotted (B) with observed results (colored points) overlaid*
246 *on the distribution of simulated data (gray violins). One star indicates that observed data is above*
247 *the 95th percentile of the distribution; two stars indicates that observed data is above the 99th*
248 *percentile. (C) Representative immunohistochemistry images of swine left apical lung section*
249 *stained for WT (green) and VAR (red) viruses at day 3 post-inoculation. Gray staining marks*
250 *epithelial cell borders. Yellow coloring in merged images indicates the presence of both WT and*
251 *VAR HA antigens in the same cell. Zoomed insets of the lung are shown with white arrows*
252 *indicating co-infected cells and yellow arrows indicating singly infected cells.*
253
254 **Discussion**
255 By monitoring reassortment between highly similar co-infecting viruses, we can detect the
256 diversity generated through genetic exchange in the absence of selection. Consequently, our
257 experiments reveal the extent to which co-infection at the level of the whole host creates
258 opportunity for reassortment within the host. Abundant opportunity is apparent in the nasal
259 tracts of guinea pigs and ferrets. However, the viral diversity generated through reassortment is
260 more limited in the lungs of ferrets and all tissues sampled in pigs. In addition to relatively little
261 opportunity for reassortment in these tissues, spatial constraints on mixing within the respiratory
262 tract yield localized sub-populations with diminished genotypic diversity. Thus, despite the
263 extensive reassortment seen among swine IAV at a population level, our results reveal only
264 moderate viral diversity generated through reassortment in pigs. Results from guinea pigs and
265 ferrets suggest that opportunity for within-host IAV genetic exchange may be greater in other
266 natural mammalian hosts.
267 Given our use of well-matched parental viruses, we can assume that the differences in viral
268 genotypic diversity seen between species and between tissues within a species are not driven by
269 natural selection. Instead, features of viral dynamics in these different environments likely shape
270 the frequency of reassortment and the extent to which reassortants are amplified once formed.
271 For example, the efficiency of viral replication, spatial arrangement of target cells, the extent to

272 which permissive cells are interspersed with non-permissive cells, physical barriers to viral spread
273 and the effectiveness innate responses to infection are all likely to vary with species and across
274 different tissues within a species[31-33].
275 Although variation in the diversity generated through reassortment is apparent, visualization of
276 viral antigen in infected tissues indicated that cellular co-infection is abundant at all sites
277 examined. Cellular co-infection has previously been reported to be common *in vivo*[34] and is
278 expected owing to the high potential for singular genomes to result in abortive infection[35,36] and
279 the potential for direct cell-to-cell spread of viral genetic material[37]. Nevertheless, the
280 juxtaposition of this result with a predominance of parental-type viruses in many samples is
281 counter-intuitive. While the images of fixed tissue show a snapshot of viral HA protein expression
282 in defined cells at a given time point, viral samples draw from the population of viruses that have
283 accumulated at a particular site over the course of infection. Thus, the prevalence of parental
284 genotypes may reflect their production early after inoculation, when cellular co-infection is less
285 likely to occur[22,34]. In addition, HA staining does not reveal the relative dosage of WT and VAR
286 genomes in a cell or indicate the genotype(s) of the seven non-HA segments. Both factors would
287 strongly modulate the proportion of progeny genomes from a co-infected cell that are
288 reassortant.
289 The spatial separation of viral sub-populations within an individual has important evolutionary
290 implications. First, reassortment among genetically distinct viruses is less likely to occur when
291 viral dispersal is localized, since all viruses produced from a singly infected progenitor cell will be
292 genetically similar[23]. Conversely, well-mixed viral populations are more likely to produce
293 reassortants that differ from their parents in biologically meaningful ways. Compartmentalization
294 of variants may be a contributing factor to the lack of reassortment reported in experimentally
295 infected humans[38]. Second, spatial structure impacts the extent to which a viral population within
296 a host is shaped by selection versus stochastic processes[39]. Spatial barriers create
297 subpopulations, each of which can have a small population size. As such, genetic drift dominates
298 within each subpopulation, with variant frequencies changing over time largely due to chance.
299 This means that both lower and higher fitness variants have the potential to rise to high
300 frequencies within subpopulations. As a result, spatial compartmentalization of populations has

301 the immediate effect of reducing the efficiency of selection. While the strength of selection to
302 purge low fitness variants is weakened at the level of individual subpopulations, the propagation
303 of slightly deleterious mutants allows a broader exploration of sequence space across the entire
304 viral population that is distributed within the host. This may, in rare cases, lead to the discovery
305 of higher fitness variants that might not evolve as readily in less structured within-host
306 populations.
307 Compartmentalization of viral replication is also expected to shape evolution occurring between
308 hosts. As has been seen in ferrets, transmitted virus is likely to comprise a sub-sample of one
309 specific anatomical location[23,40,41]. In the context of spatial heterogeneity, this sub-sample will
310 not be representative of the viral population present in the whole host. Thus, within-host spatial
311 structure is expected to contribute to stochastic effects acting between hosts: the transmitted
312 virus will be the virus that was in the right place at the right time, and may not be the most fit
313 genotype present within a host[23,41-43].
314 Certain limitations in our experimental design are important to consider. Our approach of co-
315 inoculating with well-matched parental strains is designed to maximize potential to detect
316 reassortment. In addition, the gene constellation of the 2009 pandemic H1N1 virus, used in this
317 study, has shown a marked predisposition for reassortment[44-46]. However, natural co-infections
318 will include a wide range of scenarios in terms of relative timing, route and dose of infection and
319 phenotypes of co-infecting strains. Each of these factors will influence the frequency of
320 reassortment[21-23,47]. In evaluating the extent of overlap between viral genotypes in different
321 anatomical locations, it is important to note that parental viruses are likely seeded throughout
322 the respiratory tract upon inoculation; thus, only reassortant genotypes are informative in
323 assessing the extent of mixing across sites. In addition, if variants are rare (<5%), they would fall
324 below the limit of detection of our assay.
325 IAV reassortment within cells is efficient, such that 256 distinct genotypes are readily formed in
326 a single co-infected cell[48]. However, within a host, the high potential for reassortment to
327 generate diversity is subject to complex dynamics that define the likelihood of cellular co-
328 infection and the extent to which novel reassortants are propagated. While our data reveal
329 extensive co-infection *in vivo* and consistent formation of reassortants, species and tissue

330 differences in the extent of reassortment are apparent. Spatial constraints on the dissemination
331 of novel genotypes add to this complexity and are likely to be a major factor in within-host viral
332 evolutionary dynamics.
333
334 **Author Contributions**
335 KG contributed to the conception of work, experimental design, data acquisition and analysis,
336 interpretation of data; AB contributed to data analysis, model development and interpretation
337 of data; LMF, GG, SC, CJC, BS, YL, LW, TK, YL and IM contributed to data acquisition; WM, JAR and
338 DRP contributed to conception of the work, experimental design, data analysis and
339 interpretation; KK contributed to conception of the work, data analysis and interpretation; ACL
340 contributed to conception of work, experimental design and data analysis and interpretation. All
341 authors contributed to the writing of the manuscript.
342
343 **Conflict of interest statement**
344 The JAR laboratory received support from Tonix Pharmaceuticals, Xing Technologies and Zoetis,
345 outside of the reported work. JAR is inventor on patents and patent applications on the use of
346 antivirals and vaccines for the treatment and prevention of virus infections, owned by Kansas
347 State University, KS.
348
349 **Methods**
350 **Cells and cell culture media.** Madin–Darby canine kidney (MDCK) cells, a gift from Dr. Robert
351 Webster, St Jude Children's Research Hospital, Memphis, TN to D.R.P were used for all
352 experiments. A seed stock of MDCK cells at passage 23 was subsequently amplified and
353 maintained in Minimal Essential Medium (Gibco) supplemented with 10% fetal bovine serum
354 (FBS; Atlanta Biologicals) and Normocin (Invivogen). 293T cells (ATCC, CRL-3216) were
355 maintained in Dulbecco's Minimal Essential Medium (Gibco) supplemented with 10% FBS and PS.
356 All cells were cultured at 37°C and 5% CO_2 in a humidified incubator. The cell lines were not
357 authenticated. All cell lines were tested monthly for mycoplasma contamination while in use. The

358 medium for the culture of IAV in MDCK cells (virus medium) was prepared by supplementing the
359 basal medium for the relevant cell type with 4.3% BSA and Normocin.
360
361 **Viruses.** Viruses used in this study were derived from influenza A/Netherlands/602/2009 (H1N1)
362 virus (NL09) and were generated by reverse genetics[49-51]. In brief, 293T cells transfected with
363 reverse-genetics plasmids 16–24 h previously were co-cultured with MDCK cells at 37°C for 40–
364 48 h. Recovered virus was propagated in MDCK cells at a low multiplicity of infection to generate
365 working stocks. Titration of stocks and experimental samples was carried out by plaque assay in
366 MDCK cells. Silent mutations were introduced into each segment of the VAR virus by site-directed
367 mutagenesis of reverse genetics plasmids. The specific changes introduced into the VAR virus
368 were reported previously[24,28]. NL09 VAR virus was engineered to contain a 6XHIS epitope tag plus
369 a GGGS linker at the amino (N) terminus of the HA protein following the signal peptide. NL09 WT
370 virus carries an HA epitope tag plus a GGGS linker inserted at the N terminus of the HA protein[28].
371 A 1:1 mixture of NL09 WT and VAR viruses was prepared using methods described previously[24].
372
373 **Animal models and reassortment *in vivo*.** All the animal experiments were conducted in
374 accordance with the Guide for the Care and Use of Laboratory Animals of the National Institutes
375 of Health. The studies were conducted under animal biosafety level 2 containment and approved
376 by the IACUC of Emory University (DAR-2002738-ELMNTS-A) for guinea pig (*Cavia porcellus*), the
377 IACUC of the University of Georgia (AUP A2015 06-026-Y3-A5) for ferret (*Mustela putorius furo*)
378 and the IACUC of Kansas State University (protocol #4120) for swine (*Sus scrofa*). The animals
379 were humanely euthanized following guidelines approved by the American Veterinary Medical
380 Association.
381 Female, Hartley strain guinea pigs weighing 250–350 g were obtained from Charles River
382 Laboratories and housed by Emory University Department of Animal Resources. Before intranasal
383 inoculation and nasal washing, the guinea pigs were anaesthetized with 30 mg kg^{-1} ketamine and
384 4 mg kg^{-1} xylazine by intramuscular injection. The $GPID_{50}$ of the NL09 virus was previously
385 determined to be $1x10^1$ PFU[29]. To evaluate reassortment kinetics in guinea pigs, groups of six
386 animals were infected with $1x10^3$ PFU ($1x10^2$ ID_{50}) or $1x10^6$ PFU ($1x10^5$ ID_{50}) of the NL09 WT/VAR

387 virus mixtures. Virus inoculum was given intranasally in a 300 µl volume of PBS. Nasal washes
388 were performed on days 1–6 post-inoculation and titered by plaque assay. Viral genotyping was
389 performed on samples collected on days 1, 2 and 3 or 4 for each guinea pig. Day 3 was used for
390 animals receiving the higher dose since virus is cleared rapidly in this system and shedding has
391 ceased by day 4.
392 Female ferrets, 20-weeks-old, from Triple F Farms (Gillett, PA) were used. All ferrets were
393 seronegative by anti-nucleoprotein (anti-NP) influenza virus enzyme-linked immunosorbent
394 assay, Swine Influenza Virus Ab Test, (IDEXX, Westbrook, ME) prior to infection. Five days prior
395 to experimentation, ferrets were sedated, and a subcutaneous transponder (Bio Medic Data
396 Systems, Seaford, Delaware) was implanted to identify each animal and provide temperature
397 readings. Anesthetics were applied via intramuscular injection with ketamine (20 mg kg^{-1}) and
398 xylazine (1 mg kg^{-1}). Infections were performed via intranasal inoculation of 1 mL of virus diluted
399 in PBS. Ferret nasal washes were carried out as follows. Ferrets were anesthetized and 1 ml of
400 PBS administered to the nose was used to induce sneezing. Expelled fluid was collected into Petri
401 dishes and samples were collected in an additional volume of 1 mL PBS. Infected ferrets were
402 monitored daily for clinical signs, temperature and weight loss. Ferrets were euthanized by
403 intravenous injection of 1 ml of Beuthanasia-D diluted 1:1 with DI water (Merck, Madison, NJ).
404 For determination of ferret ID_{50}, six groups of four ferrets each were inoculated with increasing
405 doses of the NL09 WT/VAR virus mixture ($1x10^{0.1}$ PFU, $1x10^{0}$ PFU, $1x10^{1}$ PFU, $1x10^{2}$ PFU, $1x10^{3}$
406 PFU and $1x10^{4}$ PFU). Nasal washes were collected daily for up to 6 days and titrated for viral
407 shedding by plaque assay. The ferret ID_{50} was determined based on results obtained at day 2 and
408 found to be equivalent to 3.2×10^{2} PFU.
409 For analysis of reassortment frequency and detection of viral antigen in tissues, ferrets were
410 inoculated with 3.2×10^{4} PFU ($1x10^{2}$ ID_{50}) or 3.2×10^{7} PFU ($1x10^{5}$ ID_{50}). After infections, nasal
411 washes were collected daily for up to 6 days and titrated by plaque assay. Viral genotyping was
412 performed on samples collected on days 1, 3 and 5 for each ferret. Tissue sections collected for
413 virology were disrupted in 1 mL of sterile PBS using the TissueLyser LT (Qiagen, Germantown,
414 MD) at 30 Hz for 5 min twice, in microcentrifuge tubes with 3 mm Tungsten Carbide Beads
415 (Qiagen, St. Louis, MO). Supernatants were clarified by centrifugation and frozen at -80 ºC until

416 viral titration. For histology, tissues were submerged in 10% buffered formalin (Sigma Aldrich, St.
417 Louis, MO) and stored at room temperature until evaluation.
418 The pig study was conducted at the Large Animal Research Center (a biosafety level 2+ facility)
419 at Kansas State University in accordance with the Guide for the Care and Use of Agricultural
420 Animals in Research and Teaching of the U.S. Department of Agriculture. To determine virus
421 reassortment and viral antigen in tissues, eighteen 4-week-old influenza H1 and H3 subtype virus-
422 and porcine reproductive and respiratory syndrome virus-seronegative gender-mixed crossbred
423 pigs were randomly allocated into groups. Each pig was inoculated with 2 x 10^6 PFU of NL09
424 WT/VAR mixture through both intranasal and intratracheal routes (10^6 PFU was administered in
425 a 1 ml volume by each of these two routes) under anaesthesia as described previously[52]. Clinical
426 signs for all experimental pigs were monitored daily throughout the experiment. Nasal swabs
427 were collected at 1, 3, 5 and 7 days post infection from each pig. Three infected pigs were
428 euthanized at 3-, 5-, and 7-days post infection. During necropsy, nasal turbinate, trachea and lung
429 tissues from 7 lobes collected from each pig were frozen at -80°C for virus isolation and fixed in
430 10% buffered formalin for IHC examination.
431
432 **Quantification of reassortment.** Reassortment frequencies were evaluated by genotyping 21
433 clonal viral isolates per sample as described previously[48]. This analysis was applied to guinea pig
434 nasal washes, ferret nasal washes, swine nasal swabs, ferret tissue homogenates and swine tissue
435 homogenates. Time points to be examined were chosen based on positivity in all animals in a
436 treatment group. Thus, samples from days 1, 2, 3 or 4 were evaluated from guinea pigs, while
437 samples from days 1, 3 and 5 were evaluated for ferrets and swine. The genotypes of virus
438 isolates detected in all samples analysed are reported in Supplementary Table 1.
439 Briefly, plaque assays were performed on MDCK cells in 10 cm dishes to isolate virus clones.
440 Serological pipettes (1 ml) were used to collect agar plugs into 160 µl PBS. Using a ZR-96 viral RNA
441 kit (Zymo), RNA was extracted from the agar plugs and eluted in 40 µl nuclease-free water
442 (Invitrogen). Reverse transcription was performed using Maxima reverse transcriptase (RT;
443 ThermoFisher) according to the manufacturer's protocol. The resulting cDNA was diluted 1:4 in
444 nuclease-free water and each cDNA was combined with segment-specific primers[24,28] designed

445 to amplify a region of approximately 100 base pairs. The amplicon for each segment contains the
446 site of the single nucleotide change in the VAR virus. Quantitative PCR was performed with
447 Precision Melt Supermix (Bio-Rad) using a CFX384 Touch Real-Time PCR Detection System (Bio-
448 Rad). Template amplification was followed by high-resolution melt analysis to differentiate the
449 WT and VAR amplicons[53]. Precision Melt Analysis software (Bio-Rad) was used to determine the
450 parental origin of each gene segment based on the melting properties of the cDNA amplicons
451 relative to WT and VAR controls. Each plaque was assigned a genotype based on the combination
452 of WT and VAR genome segments, with two variants on each of eight segments allowing for 256
453 potential genotypes. Occasionally, a gene segment cannot be typed with confidence and is
454 recorded as neither WT nor VAR. Viral isolates with ambiguous gene segments were excluded
455 from our subsequent analyses.
456
457 **Immunohistochemistry and imaging.** Tissue samples from nasal turbinates of ferrets, the right
458 caudal lung lobe of ferrets and all seven lung lobes of swine were fixed in 10% neutral buffered
459 formalin for at least 24 h before being embedded in paraffin. Nasal turbinates were decalcified
460 prior to being embedded in paraffin. Sections from all the tissues were cut and slides were
461 prepared. The tissues were deparaffinized by warming the slides at 60°C on a slide warmer for
462 45 min followed by immersion in xylenes (Sigma) for 25 min. The slides were then immersed in
463 100% ethanol for 10 min, 95% ethanol for 10 min and 70% ethanol for 5 min. The slides were
464 then washed by placing in deionized water for 1 h. Antigen retrieval was performed by steaming
465 the slides in 10 mM citric acid, pH 6.0 for 45 min, followed by washing in tap water and 1X PBS
466 (Corning) for 5 min. The WT and VAR viruses were detected in the tissues using a mouse anti HA
467 Alexa Fluor 488 (Invitrogen catalogue number A-21287; clone 16B12) and mouse anti His Alexa
468 Fluor 555 (Invitrogen catalogue number MA1-135-A555; clone 4E3D10H2/E3) while epithelial cell
469 borders were stained using rabbit anti $Na^{+}K^{+}$ ATPase Alexa Fluor 647 (Abcam catalogue number
470 198367; clone EP1845Y) at 4°C overnight. Slides were washed three times in 1X PBS (Corning)
471 and once in deionized water to remove excess antibody. The slides were mounted onto glass
472 coverslips using ProLong Diamond Anti Fade mounting media (ThermoFisher). The images were
473 acquired using an Olympus FV1000 Confocal Microscope at 60x magnification under an oil

474 immersion objective. The specificity of the antibodies was confirmed by infecting MDCK cells with
475 either the NL09 WT, NL09 VAR or both viruses for 24 h. The cells were fixed using 4%
476 paraformaldehyde (Alfa Aesar) and stained for HA and His tags using the antibodies as described
477 above (Supp Fig 5).
478
479 **Software**
480 Figures were generated using Python 3[54] and the packages matplotlib[55], NumPy[56], pandas[57] and
481 seaborn[58]. Simulations were conducted in Python 3.
482
483 **Analysis of genotype frequencies, richness and diversity**
484 Here a viral genotype is defined as a unique combination of the eight IAV segments, where each
485 segment is derived from either the variant or wild type parental virus; therefore, there are 2^8
486 possible unique genotypes, with two parental genotypes and 254 reassortant genotypes. For any
487 given sample, the frequency of each unique genotype can be calculated by dividing the number
488 of appearances each unique genotype has in the sample by the total number of clonal isolates
489 obtained for that sample.
490 Understanding the distribution of unique genotypes involves using both unweighted and
491 weighted genotype frequency statistics. Genotype richness (S) does not incorporate genotype
492 frequency and is given by the number of unique genotypes in a sample. Given our sample size of
493 21 plaque isolates, genotype richness, or the number of distinct genotypes detected in a sample,
494 can range from a minimum of 1 (a single genotype is detected 21 times) to a maximum of 21 (21
495 unique genotypes are detected).
496 Diversity was measured using the Shannon-Weiner index (*H*), which considers both richness and
497 evenness in the frequency with which genotypes are detected. In our dataset, diversity can range
498 from 0 to 3.04. Shannon-Wiener diversity was calculated as:

499 $$H = -\sum_{i=1}^{S}(p_i * lnp_i)\sum_{i=1}^{S}(p_i \times \ln(p_i)$$

500 where S is genotype richness and p_i is the frequency of unique genotype i in the sample (6).
501

502 To evaluate the extent to which the spatial dynamics of viral reassortment and propagation shape
503 the overall richness and diversity in a host, we sought to compare the observed richness and
504 diversity at each anatomical site to that which would be expected if virus moves freely among
505 anatomical locations. Thus, to simulate free mixing within the host, we randomly shuffled
506 observed viral genotypes among all sites in a given animal. The average richness and Shannon-
507 Wiener index of the simulated viral populations at each site were then calculated. The 5th and
508 95th percentiles for the simulated distribution of each animal were calculated and compared to
509 the observed richness and diversity for each of the anatomical sites. If a site's observed richness
510 and diversity fell below the 5th percentile or above the 95th percentile, then a barrier to the influx
511 or efflux of reassortant genotypes from or to the other sites is suggested.
512
513 **Analysis of beta diversity**
514 The dissimilarity between populations can be measured by beta diversity. For this study, we
515 evaluated beta diversity from a richness perspective, focusing on dissimilarity in the unique
516 genotypes detected and excluding consideration of their frequency. This approach was used to
517 de-emphasize the effects of WT and VAR parental genotypes, which were likely seeded into all
518 anatomical locations at the time of inoculation. We calculate the beta diversity by treating the
519 viral genotypes in two lobes as two distinct populations:

520 $$\beta = \frac{S_{1+2}}{\frac{1}{2}(S_1 + S_2)}$$

521 where S_{1+2} is the richness of a hypothetical population composed of pooling the viral genotypes
522 of the two lobes while $\frac{1}{2}(S_1 + S_2)$ represents the mean richness of the lobes
523 (7). The beta diversity of a single comparison can be normalized so that it ranges from zero to
524 one:

525 $$BD' = \frac{BD - 1}{BD_{max} - 1}\beta_n = \frac{\beta - 1}{\beta_{max} - 1}$$

526 where $BD_{max}\beta_{max}$ is the beta diversity calculated by assuming that there are no viral genotypes
527 shared by both lobes (7). A $BD'\beta_n$ closer to one indicates that the lobes' viral populations are
528 more dissimilar while a $BD'\beta_n$ closer to zero suggests that the lobes have similar unique viral

529 genotypes and overall viral richness. A $BD'\ \beta_n$ of zero occurs when all unique genotypes present
530 in one lobe are also present in the other.
531 To simulate free mixing between two lobes, we randomly shuffled the genotypes between each
532 of the 28 pairwise combinations among pig tissues and the single ferret lung-NT combination and
533 computed the $BD'\beta_n$ for each comparison. Free mixing for all combinations was simulated 1000
534 times. We reasoned that if compartmentalization was present in the observed dataset, then the
535 dissimilarity values would fall at the high end of the simulated distribution (>95th percentile).
536

537 **Statistical measures**

538 Percentiles were calculated using the percentileofscore method from the SciPy package[57]. Paired
539 t-tests and ANOVA tests were performed using the ttest_rel method and the f_oneway method
540 respectively from the SciPy Package[57].
541

542 **Data availability**

543 Raw data are included as Source Data and in Supplementary Table 1.
544

545 **Code availability**

546 Code used for data analysis and simulations is available at:
547 https://github.com/maxbagga/Influenza-A-virus-reassortment-in-mammals-gives-rise-to-spatially-
548 distinct-sub-populations
549

550 **Acknowledgements**

551 We thank Shamika Danzy for technical assistance and the Emory Division of Animal Resources for
552 their support with the guinea pig experiments. We thank Rusty Ransburgh, Baoliang Zheng,
553 Dongchang He, Abaineh Endalew, Daniel Madden, Yuekun Lang for their assistance with the pig
554 experiments. This project was supported by the Emory University Integrated Cellular Imaging
555 Microscopy Core. The research was funded by NIH R01 AI127799 and the NIH/NIAID Centers of
556 Excellence in Influenza Research and Response (CEIRR), contract numbers 75N93021C00017
557 (ACL, KK), 75N93021C00014 (DRP) and 75N93021C00016 (JAR, WM), and the AMP Core of the

558 Center of Emerging and Zoonotic Infectious Diseases (CEZID) from NIGMS under award number
559 P20GM130448 (JAR).

560 **References**

561

562 1 Webster, R. G., Hinshaw, V. S., Bean, W. J., Jr., Turner, B. & Shortridge, K. F. Influenza
563 viruses from avian and porcine sources and their possible role in the origin of human
564 pandemic strains. *Dev Biol Stand* **39**, 461-468 (1977).
565 2 Wright, P. F., Neumann, G. & Kawaoka, Y. in *Fields Virology* Vol. 1 (ed D. M. & Howley
566 Knipe, P. M.) 1691-1740 (Lippincott-Raven, 2006).
567 3 Webster, R. G., Bean, W. J., Gorman, O. T., Chambers, T. M. & Kawaoka, Y. Evolution and
568 ecology of influenza A viruses. *Microbiol Rev* **56**, 152-179 (1992).
569 4 Webster, R. G., Shortridge, K. F. & Kawaoka, Y. Influenza: interspecies transmission and
570 emergence of new pandemics. *FEMS Immunol Med Microbiol* **18**, 275-279, doi:S0928-
571 8244(97)00058-8 [pii] (1997).
572 5 Taubenberger, J. K. & Morens, D. M. 1918 Influenza: the mother of all pandemics. *Emerg*
573 *Infect Dis* **12**, 15-22 (2006).
574 6 Viboud, C., Miller, M., Olson, D., Osterholm, M. & Simonsen, L. Preliminary Estimates of
575 Mortality and Years of Life Lost Associated with the 2009 A/H1N1 Pandemic in the US and
576 Comparison with Past Influenza Seasons. *PLoS Curr*, RRN1153, doi:k/-/-
577 /35hpbywfdwl4n/8 [pii] (2010).
578 7 Ma, E. J., Hill, N. J., Zabilansky, J., Yuan, K. & Runstadler, J. A. Reticulate evolution is
579 favored in influenza niche switching. *Proc Natl Acad Sci U S A* **113**, 5335-5339,
580 doi:10.1073/pnas.1522921113 (2016).
581 8 Kilbourne, E. D. Influenza pandemics of the 20th century. *Emerg Infect Dis* **12**, 9-14 (2006).
582 9 Smith, G. J. *et al.* Origins and evolutionary genomics of the 2009 swine-origin H1N1
583 influenza A epidemic. *Nature* **459**, 1122-1125, doi:10.1038/nature08182 (2009).
584 10 Nelson, M. I. & Vincent, A. L. Reverse zoonosis of influenza to swine: new perspectives on
585 the human-animal interface. *Trends Microbiol* **23**, 142-153,
586 doi:10.1016/j.tim.2014.12.002 (2015).
587 11 Woods, G. T., Schnurrenberger, P. R., Martin, R. J. & Tompkins, W. A. Swine influenza virus
588 in swine and man in Illinois. *J Occup Med* **23**, 263-267 (1981).
589 12 Ma, W. *et al.* Identification of H2N3 influenza A viruses from swine in the United States.
590 *Proc Natl Acad Sci U S A* **104**, 20949-20954, doi:10.1073/pnas.0710286104 (2007).
591 13 Ma, W., Kahn, R. E. & Richt, J. A. The pig as a mixing vessel for influenza viruses: Human
592 and veterinary implications. *J Mol Genet Med* **3**, 158-166 (2008).
593 14 Kahn, R. E., Ma, W. & Richt, J. A. Swine and influenza: a challenge to one health research.
594 *Curr Top Microbiol Immunol* **385**, 205-218, doi:10.1007/82_2014_392 (2014).
595 15 Rajao, D. S. *et al.* Reassortment between Swine H3N2 and 2009 Pandemic H1N1 in the
596 United States Resulted in Influenza A Viruses with Diverse Genetic Constellations with
597 Variable Virulence in Pigs. *J Virol* **91**, doi:10.1128/JVI.01763-16 (2017).
598 16 Nelson, M. I. *et al.* Genomic reassortment of influenza A virus in North American swine,
599 1998-2011. *J Gen Virol* **93**, 2584-2589, doi:10.1099/vir.0.045930-0 (2012).

600 17 Lam, T. T. *et al.* Reassortment events among swine influenza A viruses in China:
601 implications for the origin of the 2009 influenza pandemic. *J Virol* **85**, 10279-10285,
602 doi:10.1128/JVI.05262-11 (2011).
603 18 Zhou, N. N. *et al.* Genetic reassortment of avian, swine, and human influenza A viruses in
604 American pigs. *J Virol* **73**, 8851-8856, doi:10.1128/JVI.73.10.8851-8856.1999 (1999).
605 19 Ma, J. *et al.* Virus survival and fitness when multiple genotypes and subtypes of influenza
606 A viruses exist and circulate in swine. *Virology* **532**, 30-38, doi:10.1016/j.virol.2019.03.016
607 (2019).
608 20 Ganti, K. *et al.* Avian Influenza A Viruses Reassort and Diversify Differently in Mallards and
609 Mammals. *Viruses* **13**, doi:10.3390/v13030509 (2021).
610 21 Tao, H., Li, L., White, M. C., Steel, J. & Lowen, A. C. Influenza A Virus Coinfection through
611 Transmission Can Support High Levels of Reassortment. *J Virol* **89**, 8453-8461,
612 doi:10.1128/JVI.01162-15 (2015).
613 22 Tao, H., Steel, J. & Lowen, A. C. Intrahost dynamics of influenza virus reassortment. *J Virol*
614 **88**, 7485-7492, doi:10.1128/JVI.00715-14 (2014).
615 23 Richard, M., Herfst, S., Tao, H., Jacobs, N. T. & Lowen, A. C. Influenza A Virus Reassortment
616 Is Limited by Anatomical Compartmentalization following Coinfection via Distinct Routes.
617 *J Virol* **92**, doi:10.1128/JVI.02063-17 (2018).
618 24 Phipps, K. L. *et al.* Collective interactions augment influenza A virus replication in a host-
619 dependent manner. *Nat Microbiol* **5**, 1158-1169, doi:10.1038/s41564-020-0749-2 (2020).
620 25 Belser, J. A., Katz, J. M. & Tumpey, T. M. The ferret as a model organism to study influenza
621 A virus infection. *Dis Model Mech* **4**, 575-579, doi:10.1242/dmm.007823 (2011).
622 26 Danzy, S., Lowen, A. C. & Steel, J. A quantitative approach to assess influenza A virus
623 fitness and transmission in guinea pigs. *J Virol*, doi:10.1128/JVI.02320-20 (2021).
624 27 Lowen, A. C., Bouvier, N. M. & Steel, J. Transmission in the guinea pig model. *Curr Top*
625 *Microbiol Immunol* **385**, 157-183, doi:10.1007/82_2014_390 (2014).
626 28 Phipps, K. L. *et al.* Seasonal H3N2 and 2009 Pandemic H1N1 Influenza A Viruses Reassort
627 Efficiently but Produce Attenuated Progeny. *J Virol* **91**, doi:10.1128/JVI.00830-17 (2017).
628 29 Campbell, P. J. *et al.* The M segment of the 2009 pandemic influenza virus confers
629 increased neuraminidase activity, filamentous morphology, and efficient contact
630 transmissibility to A/Puerto Rico/8/1934-based reassortant viruses. *J Virol* **88**, 3802-3814,
631 doi:10.1128/JVI.03607-13 (2014).
632 30 Jasinska, W. *et al.* Chromosomal barcoding of E. coli populations reveals lineage diversity
633 dynamics at high resolution. *Nat Ecol Evol* **4**, 437-452, doi:10.1038/s41559-020-1103-z
634 (2020).
635 31 Matrosovich, M. N., Matrosovich, T. Y., Gray, T., Roberts, N. A. & Klenk, H. D. Human and
636 avian influenza viruses target different cell types in cultures of human airway epithelium.
637 *Proc Natl Acad Sci U S A* **101**, 4620-4624, doi:10.1073/pnas.0308001101 (2004).
638 32 van Riel, D. *et al.* Novel avian-origin influenza A (H7N9) virus attaches to epithelium in
639 both upper and lower respiratory tract of humans. *Am J Pathol* **183**, 1137-1143,
640 doi:10.1016/j.ajpath.2013.06.011 (2013).
641 33 Mifsud, E. J., Kuba, M. & Barr, I. G. Innate Immune Responses to Influenza Virus Infections
642 in the Upper Respiratory Tract. *Viruses* **13**, doi:10.3390/v13102090 (2021).

643 34 Brooke, C. B., Ince, W. L., Wei, J., Bennink, J. R. & Yewdell, J. W. Influenza A virus
644 nucleoprotein selectively decreases neuraminidase gene-segment packaging while
645 enhancing viral fitness and transmissibility. *Proc Natl Acad Sci U S A* **111**, 16854-16859,
646 doi:10.1073/pnas.1415396111 (2014).
647 35 Brooke, C. B. *et al.* Most influenza a virions fail to express at least one essential viral
648 protein. *J Virol* **87**, 3155-3162, doi:10.1128/JVI.02284-12 (2013).
649 36 Jacobs, N. T. *et al.* Incomplete influenza A virus genomes occur frequently but are readily
650 complemented during localized viral spread. *Nat Commun* **10**, 3526, doi:10.1038/s41467-
651 019-11428-x (2019).
652 37 Ganti, K., Han, J., Manicassamy, B. & Lowen, A. C. Rab11a mediates cell-cell spread and
653 reassortment of influenza A virus genomes via tunneling nanotubes. *PLoS Pathog* **17**,
654 e1009321, doi:10.1371/journal.ppat.1009321 (2021).
655 38 Sobel Leonard, A. *et al.* The effective rate of influenza reassortment is limited during
656 human infection. *PLoS Pathog* **13**, e1006203, doi:10.1371/journal.ppat.1006203 (2017).
657 39 Gallagher, M. E., Brooke, C. B., Ke, R. & Koelle, K. Causes and Consequences of Spatial
658 Within-Host Viral Spread. *Viruses* **10**, doi:10.3390/v10110627 (2018).
659 40 Lakdawala, S. S. *et al.* The soft palate is an important site of adaptation for transmissible
660 influenza viruses. *Nature* **526**, 122-125, doi:10.1038/nature15379 (2015).
661 41 Xie, C. *et al.* A(H1N1)pdm09 Influenza Viruses Replicating in Ferret Upper or Lower
662 Respiratory Tract Differed in Onward Transmission Potential by Air. *J Infect Dis* **225**, 65-
663 74, doi:10.1093/infdis/jiab286 (2022).
664 42 Zaraket, H. *et al.* Mammalian adaptation of influenza A(H7N9) virus is limited by a narrow
665 genetic bottleneck. *Nat Commun* **6**, 6553, doi:10.1038/ncomms7553 (2015).
666 43 Zwart, M. P. & Elena, S. F. Matters of Size: Genetic Bottlenecks in Virus Infection and Their
667 Potential Impact on Evolution. *Annu Rev Virol* **2**, 161-179, doi:10.1146/annurev-virology-
668 100114-055135 (2015).
669 44 Vijaykrishna, D. *et al.* Reassortment of pandemic H1N1/2009 influenza A virus in swine.
670 *Science* **328**, 1529, doi:10.1126/science.1189132 (2010).
671 45 Mine, J., Uchida, Y., Takemae, N. & Saito, T. Genetic Characterization of Influenza A
672 Viruses in Japanese Swine in 2015 to 2019. *J Virol* **94**, doi:10.1128/JVI.02169-19 (2020).
673 46 Gao, S. *et al.* The genomic evolution of H1 influenza A viruses from swine detected in the
674 United States between 2009 and 2016. *J Gen Virol* **98**, 2001-2010,
675 doi:10.1099/jgv.0.000885 (2017).
676 47 White, M. C. & Lowen, A. C. Implications of segment mismatch for influenza A virus
677 evolution. *J Gen Virol* **99**, 3-16, doi:10.1099/jgv.0.000989 (2018).
678 48 Marshall, N., Priyamvada, L., Ende, Z., Steel, J. & Lowen, A. C. Influenza virus reassortment
679 occurs with high frequency in the absence of segment mismatch. *PLoS Pathog* **9**,
680 e1003421, doi:10.1371/journal.ppat.1003421 (2013).
681 49 Fodor, E. *et al.* Rescue of influenza A virus from recombinant DNA. *J Virol* **73**, 9679-9682,
682 doi:10.1128/JVI.73.11.9679-9682.1999 (1999).
683 50 Hoffmann, E., Neumann, G., Hobom, G., Webster, R. G. & Kawaoka, Y. "Ambisense"
684 approach for the generation of influenza A virus: vRNA and mRNA synthesis from one
685 template. *Virology* **267**, 310-317, doi:10.1006/viro.1999.0140 (2000).

686 51 Chutinimitkul, S. *et al.* Virulence-associated substitution D222G in the hemagglutinin of
687 2009 pandemic influenza A(H1N1) virus affects receptor binding. *J Virol* **84**, 11802-11813,
688 doi:10.1128/JVI.01136-10 (2010).
689 52 Richt, J. A. *et al.* Pathogenic and antigenic properties of phylogenetically distinct
690 reassortant H3N2 swine influenza viruses cocirculating in the United States. *J Clin*
691 *Microbiol* **41**, 3198-3205, doi:10.1128/JCM.41.7.3198-3205.2003 (2003).
692 53 Wittwer, C. T., Reed, G. H., Gundry, C. N., Vandersteen, J. G. & Pryor, R. J. High-resolution
693 genotyping by amplicon melting analysis using LCGreen. *Clin Chem* **49**, 853-860,
694 doi:10.1373/49.6.853 (2003).
695 54 Van Rossum, G. & Drake, F. L. *Python 3 Reference Manual*. (CreateSpace, 2009).
696 55 Hunter, J. D. Matplotlib: A 2D Graphics Environment. *Computing in Science & Engineering*
697 **9**, 90-95, doi:doi: 10.1109/MCSE.2007.55 (2007).
698 56 Oliphant, T. E. *A guide to NumPy* Vol. 1 (Trelgol Publishing, 2006).
699 57 McKinney, W. Data structures for statistical computing in python. *Proceedings of the 9th*
700 *Python in Science Conference* **445**, 51-56 (2010).
701 58 Waskom, M. L. seaborn: statistical data visualization. *Journal of Open Source Software* **6**,
702 3021, doi:doi:10.21105/joss.03021 (2021).
703

704

705 **Figure Legends**

706 **Figure 1: Viral genotypic diversity generated through reassortment in the mammalian nasal**
707 **tract.** Results from guinea pigs are shown in panels A–D, ferrets in panels E–H and swine in panels
708 I-L. Stacked plots (A, E, I) show frequencies of unique genotypes detected in one representative
709 animal over time. Blue and orange represent the WT and VAR parental genotypes, respectively.
710 Frequency of both parental genotypes combined (B, F, J), richness (C, G, K) and Shannon-Weiner
711 diversity (D, H, L) are each plotted as a function of time. Guinea pigs and ferrets inoculated at
712 high dose ($1x10^5$ ID_{50}) and low dose ($1x10^2$ ID_{50}) are indicated with dashed and solid lines,
713 respectively. The distribution of parental genotype frequencies (M), richness (N) and diversity (O)
714 across all time points in each species is shown with violin plots. Differences in richness and
715 diversity between swine and guinea pigs and between swine and ferrets were significant ($p<0.01$,
716 ANOVA). Parental genotype frequencies differed significantly between swine and guinea pigs
717 ($p=0.003$, ANOVA), and were not significant between swine and ferrets (ANOVA).

718

719 **Figure 2: Viral diversity generated through reassortment is greater in the ferret nasal turbinates**
720 **than in the lungs.** Pie charts show frequencies of unique genotypes detected in the nasal

721 turbinates (NT) and lung of ferrets inoculated with $1x10^2$ FID_{50} (A) or $1x10^5$ FID_{50} (B), with the
722 blue and orange sections representing WT and VAR parental genotypes, respectively. Richness
723 (C) and diversity (D) are plotted, with observed results (colored points) overlaid on the
724 distribution of simulated data (grey violins). Dashed lines denote the 95th and 5th percentiles. The
725 distribution of richness (E) and diversity (F) in NT and lungs of all individuals is shown with violin
726 plots. Differences between NT and lungs were significant by both measures ($p<0.01$, paired t-
727 test).
728
729 **Figure 3: Reassortant viral populations in the ferret upper and lower respiratory tracts are**
730 **distinct.** Heat map showing normalized beta diversity of viral populations in ferret lung and nasal
731 turbinates (NT) (A). The inset shows a representative comparison between the tissues of ferrets
732 F23 and F21, to indicate the position of NT and lung within the matrix. Normalized beta diversity
733 is plotted in (B) with observed results (colored points) overlaid on the distribution of simulated
734 data (gray violins). One star indicates that observed data is above the 95th percentile of the
735 distribution; two stars indicates that observed data is above the 99th percentile. (C)
736 Immunohistochemistry images of ferret NT and lung sections stained for WT (green) and VAR
737 (red) viruses at day 3 post-inoculation. Gray staining marks epithelial cell borders. Yellow coloring
738 in merged images indicates the presence of both WT and VAR HA antigens in the same cell.
739 Zoomed insets of both NT and lung sections are shown with white arrows indicating co-infected
740 cells and yellow arrows indicating singly infected cells.
741
742 **Figure 4: Local diversity arising through reassortment is modest within the swine respiratory**
743 **tract.** Pie charts showing frequencies of unique genotypes present within each lung lobe of a
744 given pig on day 3 (A-C) and the nasal tract and each lung lobe of a given pig on day 5 (D-F) with
745 blue and orange sections representing WT and VAR parental genotypes, respectively. The tissue
746 sites are abbreviated as NA-Nasal; LA-Left Apical; RA-Right Apical; LC-Left Cardiac; RC-Right
747 Cardiac; LD-Left Diaphragmatic; RD-Right Diaphragmatic; IN-Intermediate. Simulated richness (G)
748 and diversity (H) are plotted, with observed results (colored points) overlaid on the distribution
749 of simulated data (grey violins). Dashed lines denote the 95th and 5th percentiles.

750

751 **Figure 5: Reassortant viral populations show extensive compartmentalization within the swine**
752 **respiratory tract.** Heat map showing normalized beta diversity of viral populations in swine lung
753 and nasal tract (A). The inset shows a representative comparison between the tissues of pigs P3
754 and P6, to indicate the position of each tissue within the matrix. The tissue sites are abbreviated
755 as NA-Nasal; LA- Left Apical; RA- Right Apical; LC-Left Cardiac; RC-Right Cardiac; LD-Left
756 Diaphragmatic; RD-Right Diaphragmatic; IN-Intermediate. Normalized beta diversity between
757 the left apical and left cardiac lobes is plotted (B) with observed results (colored points) overlaid
758 on the distribution of simulated data (gray violins). One star indicates that observed data is above
759 the 95th percentile of the distribution; two stars indicates that observed data is above the 99th
760 percentile. (C) Representative immunohistochemistry images of swine left apical lung section
761 stained for WT (green) and VAR (red) viruses at day 3 post-inoculation. Gray staining marks
762 epithelial cell borders. Yellow coloring in merged images indicates the presence of both WT and
763 VAR HA antigens in the same cell. Zoomed insets of the lung are shown with white arrows
764 indicating co-infected cells and yellow arrows indicating singly infected cells.

765

766

767 **Supplementary Figure Legends**

768

769 **Supp Fig 1. Viral genotypic diversity generated through reassortment in the mammalian nasal**
770 **tract.** Stacked plots showing frequencies of unique genotypes detected in guinea pigs (A), ferrets
771 (B) or swine (C) over time. The sections in blue and orange represent the WT and VAR parental
772 genotypes, respectively.

773

774 **Supp Fig 2. Reassortant viral populations show extensive compartmentalization within the**
775 **swine respiratory tract.** Heat maps showing beta diversity of viral populations in the lung lobes
776 and nasal tract of individual pigs. Pig ID number is indicated above each matrix. The tissue sites
777 are abbreviated as NA-Nasal; LA- Left Apical; RA- Right Apical; LC-Left Cardiac; RC-Right Cardiac;
778 LD-Left Diaphragmatic; RD-Right Diaphragmatic; IN-Intermediate.

779

780 **Supp Fig 3. Reassortant viral populations show extensive compartmentalization within the**
781 **swine respiratory tract.** Normalized beta diversity between each lung lobe and nasal tract (A)
782 and between lung lobes (B) are plotted with observed results (colored points) overlaid on the
783 distribution of simulated data (gray violins). One star indicates that observed data is above the
784 95th percentile of the distribution; two stars indicates that observed data is above the
785 99th percentile.
786
787 **Supp Fig 4. Coinfection is common in the swine respiratory tract.** Immunohistochemistry images
788 of lung tissue sections stained for WT (green) and VAR (red) viruses at day 3 post-inoculation. The
789 lung lobe sampled is indicated at the left. Gray staining marks epithelial cell borders. Yellow
790 coloring in merged images indicates the presence of both WT and VAR HA antigens in the same
791 cell. Zoomed insets are shown with white arrows indicating co-infected cells and yellow arrows
792 indicating singly infected cells.
793
794 **Supp Fig 5. Validation of the antibodies used for immunohistochemistry.** Immunofluorescence
795 images of MDCK cells stained for WT (green) and VAR (red) viruses at 24 h post infection. Gray
796 staining marks epithelial cell borders. Yellow coloring in merged images indicates the presence
797 of both WT and VAR HA antigens in the same cell.
798
799 **Supp Table 1. Genotype tables.** Viral genotypes detected in guinea pigs, ferrets and swine are
800 included. Each table corresponds to a biological sample and each row in each table corresponds
801 to a single viral isolate. The columns show the eight viral gene segments. Blue color blocks
802 indicate WT genes while red color blocks indicate VAR genes. White blocks indicate that an
803 ambiguous result was obtained for that gene segment; genotypes with missing information were
804 excluded from quantitative analyses.